DOI: 10.26599/FSHW.2026.9251043

Contents lists available at SciOpen

Food Science and Human Wellness

journal homepage: https://www.sciopen.com/journal/2097-0765

China Food Publishing Co.

Vitamin D_3 Spatially Regulates Gut Homeostasis in Obese Mice: Segmental Epithelial Integrity and Microbial Ecology

Yilong Cao, Xinyu Wu, Yixiang Liu*

College of Ocean Food and Biological Engineering, Jimei University, Xiamen, Fujian, 361021, China

ABSTRACT: Obesity is closely linked to vitamin D_3 (VD_3) deficiency and intestinal homeostasis disruption, underscoring a VD_3-gut homeostasis-obesity triad. This study investigates how VD_3 spatially regulates gut epithelial homeostasis and microbiota in high-fat diet (HFD)-induced obese mice, highlighting its significance for obesity nutritional management. Mice fed with a standard HFD served as models of diet-induced obesity and were administrated VD_3. Epithelial oxidative stress/inflammation, barrier function, and microbiota were assessed across intestinal segments to evaluate VD_3's spatially specific role in intestinal homeostasis regulation under obese physiology. It was found that VD_3 supplementation could suppress HFD-induced weight gain. Comparative analysis of duodenal, jejunal, ileal, and colonic epithelia revealed that VD_3 preferentially alleviated oxidative stress, inflammation, and barrier dysfunction in the ileum and colon: colonic pro-inflammatory cytokines decreased by 29.26–47.90%, markedly higher than in the ileum (8.68–34.18%); VD_3 upregulated ileal tight junction proteins mRNA and protein expression levels (73.26-197.62% and 66.63-199.89%) and mucin (8.68%), while balancing colonic pro-inflammatory macrophage (M1)/anti-inflammatory macrophage (M2) polarization. Gut microbiota analysis demonstrated VD_3 enriched *Lactobacillus* in the ileum and *Lachnospiraceae* in the colon, while suppressing *Faecalibaculum* and *Romboutsia*. VD_3 exhibits segment-specific gut homeostasis regulation in obesity through antioxidant, anti-inflammatory, barrier repair, and microbiota remodeling mechanisms, validating the necessity of micronutrient supplementation for obesity management.

Keywords: Micronutrient; High-fat diet; Oxidative stress; Intestinal epithelium; Bacterial flora

1. Introduction

The intestinal ecosystem maintains homeostasis through a sophisticated crosstalk between host physiology, luminal environment, and microbial metabolites[1]. Emerging clinical evidence reveals disruption of gut homeostasis initiates a pathogenic cascade characterized by compromised epithelial integrity, chronic low-grade inflammation, and metabolic endotoxemia[2-3]—hallmarks preceding obesity-related comorbidities including type 2 diabetes[4] and non-alcoholic fatty liver disease[5]. Obesity currently afflicts nearly one-third of the world's population[6]. Although traditional caloric restriction transiently ameliorates adiposity parameters, emerging metagenomic evidence reveals persistent gut homeostatic disturbances—particularly microbial dysbiosis—that endure post-weight loss, potentially accounting for

***Corresponding author**
lyxjmu@jmu.edu.cn

Received 25 May 2025
Received in revised from 4 September 2025
Accepted 20 November 2025

elevated relapse rates[7-8]. This paradox highlights the incomplete understanding of the mechanisms by which intestinal homeostatic disruption impacts obesity management.

Obesity harms overall health and increases the risk of chronic diseases. Traditional weight-loss methods and anti-obesity drugs are widely used. However, these methods and drugs have limitations, and obesity treatment has a high relapse rate. This highlights the need for better and more sustainable treatments[8]. Moreover, the vast majority of these agents focus primarily on directly targeting lipid metabolism or energy expenditure[9-11] and fail to ameliorate obesity-induced intestinal homeostasis disruption. Growing evidence indicates that obesity disrupts intestinal homeostasis, which in turn exacerbates obesity progression by altering metabolic and immune functions[4, 12]. We speculate that in obesity, the maintenance of intestinal homeostasis could benefit the control of obesity symptoms, prevent further deterioration, and serve as a supportive adjunct to other weight-loss strategies.

Obesity is often accompanied by micronutrient deficiencies, which may impair the effectiveness of lipid metabolism regulation. Vitamin D_3 (VD_3), a fat-soluble vitamin, has gained attention for its unique physiological functions. Due to altered distribution in obese individuals, VD_3 deficiency is common in people with obesity. Obesity-related chronic inflammation and metabolic disorders increase VD_3 consumption, exacerbating its deficiency[13-14]. In turn, VD_3 deficiency promotes dyslipidemia and pro-inflammatory factors, leading to chronic inflammation and accelerated obesity development[15], thereby creating a vicious cycle. Research has shown that beyond its traditional role in calcium and phosphorus metabolism, VD_3 also regulates lipid metabolism and intestinal homeostasis. It can reduce fat accumulation in high-fat diet (HFD)-induced mice and improve intestinal homeostasis in inflammatory bowel disease[15-16]. Therefore, it is important for people with obesity to supplement VD_3. However, the commonly recommended dose of VD_3 (600–800 IU/kg) is primarily aimed at healthy individuals, and this dose may be insufficient for those with obesity and VD_3 deficiency. It has been suggested that people with obesity may require higher doses to achieve serum levels comparable to those of healthy individuals[17]. Current studies indicate that increasing micronutrient supplementation doses for individuals with obesity is necessary, with numerous reports demonstrating symptom improvement through high-dose VD_3 (10000-25000 IU/kg) intervention in mice[13, 18]. We hypothesize that VD_3 plays a critical role in the management of obesity, particularly in addressing intestinal homeostasis imbalance. However, the relationship between VD_3 supplementation and intestinal homeostasis imbalance in the context of obesity remains unclear.

Current research predominantly focuses on uniform intestinal responses or broad microbial shifts, often overlooking the segment-specific physiological and immunological heterogeneity. Distinct intestinal segments exhibit unique physiological states, immune profiles, and microbiota colonization patterns, which may differentially modulate HFD-induced oxidative stress, inflammatory responses, and barrier dysfunction. In this study, we systematically investigated HFD-induced intestinal dyshomeostasis in obese mice, focusing on oxidative-inflammatory interplay, barrier integrity, and flora–host interactions. By comparing responses in the duodenum, jejunum, ileum, and colon, we examined the region-specific effects of VD_3 supplementation on

intestinal epithelial homeostasis and microbial communities in HFD-induced obese mice. This study should contribute to a deeper understanding of VD_3's nutritional functions in modulating intestinal epithelial homeostasis and promoting the structural restoration of gut microbiota, highlighting its spatially heterogeneous effects in alleviating obesity-related intestinal dysfunction.

2. Materials and methods

2.1 Materials

VD_3 (V8070, purity ≥ 98%) was obtained from Solarbio Science & Technology Co., Ltd. (Beijing, China). Assay kits for triglycerides (TG, A110-1-1), total cholesterol (TC, A111-1-1), low-density lipoprotein cholesterol (LDL-C, A113-1-1), high-density lipoprotein cholesterol (HDL-C, A112-1-1), malondialdehyde (MDA, A003-1-2), catalase (CAT, A007-1-1), and glutathione peroxidase (GSH-Px, A005-1-1) were provided by Nanjing Jiancheng Bioengineering Institute (Nanjing, China). Enzyme-linked immunosorbent assay (ELISA) kits for D-lactic acid (SBJ-M0727), mucin 2 (MUC2, SBJ-M0883), regenerating islet-derived protein 3γ (REG3γ, SBJ-M0722), interleukin-10 (IL-10, SBJ-R0786), tumor necrosis factor-α (TNF-α, SBJ-M0030), interleukin-1β (IL-1β, SBJ-M0027), and interleukin-6 (IL-6, SBJ-M0657) were supplied by SenBeiJia Biological Technology Co., Ltd. (Nanjing, China). Additionally, tissue fixative solution was obtained from Wuhan Servicebio Biotechnology Co., Ltd. (Wuhan, China).

The primer sequences for quantitative fluorescent polymerase chain reaction (qPCR) were synthesized by Sangon Biotech Co., Ltd. (DP419, Shanghai, China). RNA extraction was performed using a kit obtained from Tiangen Biotech Co., Ltd. (F0202, Beijing, China). Reagents for reverse transcription and qPCR were supplied by Lablead Biotechnology Co., Ltd. (R0202, Xiamen, China).

The BCA protein assay kit (PC0020), RIPA lysis buffer (R0010), skim milk (D8340), and ECL developing solution (PE0010) were obtained from Solarbio Science & Technology Co., Ltd. (Beijing, China). The polyvinylidene fluoride (PVDF, IPVH00010) membrane was purchased from Millipore (Massachusetts, USA), and Real Band Dual-Color Pre-Stained Protein Marker (C610210) was acquired from Sangon Biotech Co., Ltd. (Shanghai, China). β-actin Polyclonal Antibody (20536-1-AP), ZO-1 Polyclonal Antibody (21773-1-AP), Occludin Polyclonal Antibody (13409-1-AP), Claudin-1 Polyclonal Antibody (28674-1-AP) and HRP-conjugated Goat Anti-Rabbit IgG(H+L) (SA00001-2) were supplied by Proteintech Group, Inc. (Wuhan, China).

In order to avoid the influence of VD_3 in diets on this experiment, we customized the standard diet (10% fat calories) and high-fat diet (60% fat calories) without VD_3 from Beijing HuaFuKang Bioscience Co., Ltd. (Beijing, China), and their nutrients and energy are shown in Table 1.

Table 1. Composition of the experimental diets.

Ingredient	Standard diet	High-fat diet
	Content (g/kg)	Content (g/kg)
Casein	189.6	258.4
Cystine	2.8	3.9
Corn starch	479.8	0
Maltodextrin	118.5	161.5
Sucrose	69.0	94.1
Cellulose	47.4	64.6
Soybean oil	23.7	32.4
Lard	19.0	316.6
Mineral mixture	47.4	64.6
Vitamin mixture (excluding VD_3)	0.9	1.3
Choline bitartrate	1.9	2.6
Energy		
Calories (kcal/100 g)	385	524
Protein energy supply ratio (%)	20	20
Carbohydrate energy supply ratio (%)	70	20
Fat energy supply ratio (%)	10	60

2.2 Animals and experimental design

Twenty-one male specific pathogen-free (SPF) C57BL/6J mice (20 ± 2 g, 7-week-old) were purchased from Hangzhou Medical College (Hangzhou, China), after one week of adaptive feeding with ad libitum access to water and a standard diet, the mice were subjected to subsequent experiments at 8 weeks of age. All animal handling procedures were performed in accordance with the National Institutes of Health Guidelines for the Care and Use of Laboratory Animals (NIH Publication No. 85-23 Rev. 1985) and were approved by the Institutional Animal Care and Use Committee of Animal Laboratory Center of Jimei University (Xiamen, China, No. JMU202205031). The experiment was conducted at the Animal Experiment Center of the College of Aquatic Science, Jimei University, under controlled environmental conditions (12 h light/dark cycle, 23±2°C, 50%-70% humidity).

Previous studies have shown that VD_3 at an oral dose of 15,000 IU/kg exhibited a modulatory function on lipid metabolism in obese mice [13, 15, 18-19]. Therefore, this dose was selected for use in our experiment. The dose of VD_3 administered to obese mice in this study was extrapolated, via the body size coefficient method, to a corresponding human dose for obese individuals, yielding an approximate value of 7553.29 IU per day[20]. This dosage aligns with the recommendations of the Endocrine Society Clinical Practice Guideline, which suggests a higher dose (6000–10000 IU/day) of VD_3 to treat VD_3 deficiency and maintain a 25(OH)D level above 30 ng/mL[21]. When preparing the VD_3 solution, 50 μL of anhydrous ethanol (less than 10% of the total volume) was used to facilitate the dissolution of VD_3, and the solution was then diluted with normal saline. The normal saline used in the experiment was 0.9% sterile saline, which was prepared by dissolving 7.2 g of sodium chloride in 800 mL of ultrapure water.

According to previous reports with some modifications[18], mice were randomly divided into three groups (n=5 per group): (1) Control group: fed a standard diet (10% fat energy) and gavaged with 200 μL normal saline daily; (2) Model group: fed an HFD (60% fat energy) and gavaged with 200 μL normal saline

daily; (3) VD_3 group: fed an HFD and gavaged with 200 μL VD_3 daily. Throughout the 8-week experimental period, all mice were allowed free access to food and water. Food intake was recorded daily, and body weight was measured weekly.

At the end of the experiment, mice were fasted for 24 hours, water was not restricted, blood was collected from the eyes, and serum was obtained by centrifugation at 14000 ×g for 10 minutes and stored at -80 °C. Mice were then euthanized by cervical dislocation. The liver, 4 intestinal segments (duodenum, jejunum, ileum, and colon), and epididymal fat were collected, weighed, frozen with liquid nitrogen, and stored at -80 °C for future analysis.

2.3 Analysis of the related factors in serum

The serum levels of TG, TC, LDL-C, HDL-C and D-lactic acid were tested using commercialized kits according to the manufacturer's instructions. The absorbance was measured by the microplate detection system (microplate reader) (SpectraMax M2, Molecular devices, CA, USA).

2.4 Analysis of the related factors of intestinal epithelium

The intestinal tissue was dissected, rinsed with saline, dried on filter paper, and weighed. Then, 9 times the volume of physiological saline was added according to a mass (g) to volume (mL) ratio of 1:9. The mixture was mechanically homogenized under ice bath conditions to prepare a 10% homogenate. After centrifugation at 14000 ×g for 10 minutes, the supernatant from different intestinal tissues was collected, aliquoted, and stored at -80 °C for future use. The commercialized kits were used to measure levels of MDA, CAT, GSH-Px, MUC2, REG3γ, IL-10, TNF-α, IL-1β, and IL-6 in different intestinal segments.

2.5 Histological Analysis

The pathological analysis of the tissues was conducted according to previous methods[22]. Briefly, all experimental mice were sacrificed by cervical dislocation. Immediately, we used sterile dissection knives to take the mouse livers, epididymal fat, and intestinal tissues, washed them clean with saline, and immersed them separately in a 10-fold volume of 4% paraformaldehyde fixing solution and fat-specific fixing solution for fixation and embedded in paraffin. Sample embedding, staining, sectioning, and photography were outsourced to Wuhan Bolf Biotech Co., Ltd. (Wuhan, China).

2.6 Gene expression analysis

According to previous reports with some modifications[23], we assessed the gene expression of tight junction (TJ) proteins, such as Zonula Occludens-1 (ZO-1), Occludin and Claudin-1, M1 macrophage markers Cluster of Differentiation 86 (CD86) and Interleukin-12 subunit 40 (IL-12P40), and M2 macrophage markers Cluster of Differentiation 206 (CD206) and IL-10 in the intestine by performing qPCR amplification. RNA was extracted from different intestinal segments using kits according to the manufacturer's instructions, and the concentration and purity of RNA were detected using a UV-visible near-infrared spectrophotometer (Xiamen Alspectrum Tiancheng Optoelectronics Co., Ltd., Xiamen, China). The RNA was then reverse transcribed into cDNA using a fluorescence quantitative PCR instrument (Hangzhou Langji Scientific

Instruments Co., Ltd., Hangzhou, China). Taq SYBR® Green qPCR Premix was used to perform qPCR reactions on a PCR instrument to quantify the extent of RNA expression. The 20 μL of qPCR reaction system included 4 μL cDNA, 10 μL Taq SYBR® Green qPCR Premix, 3 μL forward and reverse primers. The relative mRNA expressions were calculated by $2^{-\Delta\Delta Ct}$ using β-actin as an internal reference gene. The primer sequences used in this procedure are shown in Table 2.

Table 2. The primer sequences used in qPCR.

Gene name	Primers	Sequence (5′-3′)
ZO-1	Forward	CGG AAC TAT GAC CAT CGC CTA C
	Reverse	CTT CGG GAT GTT GTC TGG AGT C
Occludin	Forward	GTG AAT GGG TCA CCG AGG GA
	Reverse	TCC AGG CTC CCA AGA TAA GC
Claudin-1	Forward	AAA GCA CCG GGC AGA TAC AG
	Reverse	TCA TGC CAA TGG TGG ACA CA
CD86	Forward	AGC ACG GAC TTG AAC AAC CA
	Reverse	CGT CTC CAC GGA AAC AGC AT
IL-12P40	Forward	TGT GGA ATG GCG TCT CTG TC
	Reverse	AGT TCA ATG GGC AGG GTC TC
CD206	Forward	ACG AGC AGG TGC AGT TTA CA
	Reverse	ACA TCC CAT AAG CCA CCT GC
IL-10	Forward	GCT CCA AGA CCA AGG TGT CT
	Reverse	CCA AGG AGT TGT TTC CGT TAG C
β-actin	Forward	TTA CTG CTC TGG CTC CTA GC
	Reverse	CAG CTC AGT AAC AGT CCG C

2.7 Western blot analysis

The frozen intestinal tissue samples were removed from the -80°C freezer. An appropriate amount of duodenal, jejunal, ileal, and colonic tissues was weighed at a ratio of 1:100 (mg/mL) and homogenized with RIPA lysis buffer containing 1% protease inhibitor and 1% phosphatase inhibitor. The homogenate was then centrifuged at 12,000 × g for 10 minutes at 4°C to collect the protein supernatant. The protein concentration of the samples was determined using a BCA kit according to the manufacturer's instructions. The proteins were separated by 10% SDS-PAGE and subsequently transferred onto a PVDF membrane. The membrane was blocked with 5% skim milk on a shaker for 2 hours. It was then incubated overnight at 4°C with primary antibodies (ZO-1, Occludin, Claudin-1, and β-actin), followed by three washes with TBST, and further incubated with a secondary antibody for 1 hour at room temperature. An ECL developer was applied to the membrane, and imaging was performed using a chemiluminescence imaging system. The gray values of the bands were analyzed using ImageJ software.

2.8 Gut microbiota analysis

Mice were dissected in a biosafety cabinet and content-rich ileal and colonic tissue samples were collected from each group of mice, rapidly frozen in liquid nitrogen and stored at -80 °C. Microbial analysis was carried out using Majorbio Biopharm Technology Co., Ltd. (Shanghai, China). Firstly, intestinal DNA was extracted using the E.Z.N.A. soil DNA Kit. The 16S rRNA genes were amplified three times with 338F–806R primers (5′-ACTCCTACGGGAGGCAGCAG-3′ and 5′-GGACTACHVGGGTWTCTAAT-3′). Then, the PCR products were purified using the AxyPrep DNA Gel Extraction Kit, sequenced on the

Illumina MiSeq PE300 system (Illumina, San Diego, USA), and quantified with a Quantus Fluorometer (Promega, USA). Raw data underwent demultiplexing and quality filtering via Fastp (v0.20.0) and were processed in QIIME 2 (versions 2017.9 and 2018.8) following the recommended procedures.

2.9 Statistical analysis

Raw data were organized using Microsoft Excel (version 2021). Statistical analyses were performed using SPSS Statistics software (version 19). One-way analysis of variance (ANOVA) was applied for group comparisons, followed by Duncan's new multiple range test for post hoc analysis. Differences were considered statistically significant at $P < 0.05$, and significant differences among groups are indicated with different lowercase letters. All data points were included in the column graphs. Graphs were generated using OriginPro (version 9.5).

3. Results

3.1 VD_3 ameliorates HFD-fed obesity

After 8 weeks of HFD feeding with concomitant VD_3 supplementation (Figure. 1A), VD_3 showed good lipid-lowering effects in HFD-induced mice. The model group exhibited a 41.58% increase in body weight compared with the control group ($P < 0.05$), confirming the successful establishment of diet-induced obesity (Figure. 1B). Notably, VD_3-treated mice demonstrated a marked attenuation of weight gain, corroborating the macroscopic morphological observations. Energy intake did not differ between the model and VD_3 groups ($P > 0.05$). This suggests that VD_3's anti-obesity effects were not due to reduced calorie intake (Figure. 1C).

Quantitative analysis of adiposity indices revealed that VD_3 intervention significantly reduced Lee's index, Liver index, and Epididymal fat index (reductions of 8.35%, 12.25%, and 23.22%, respectively ($P < 0.05$) compared with the untreated model group (Figure. 1). Liver morphological analysis showed characteristic grayish-white discoloration in the model group, in contrast to the normal reddish-brown coloration observed in controls (Figure. 1F). Histopathological evaluation via hematoxylin-eosin (H&E) staining confirmed extensive lipid droplet accumulation in the model group, which was substantially ameliorated by VD_3 treatment (Figure. 1F). Adipose tissue analysis demonstrated significant hypertrophy of epididymal fat depots and adipocyte enlargement (Figure. 1I) in HFD-fed mice, both of which were effectively mitigated by VD_3 administration.

Serum was retrieved from the -80 °C freezer and tested for four serum lipid parameters according to the kit instructions, serum lipid profiling demonstrated that HFD feeding induced dyslipidemia, manifested by elevated TC, TG and LDL-C (increased by 23.83%, 103.08%, and 21.63%, respectively ($P < 0.05$), concomitant with reduced HDL-C (34.28%) relative to controls. Remarkably, VD_3 intervention significantly modulated lipid homeostasis, achieving a 9.87% reduction in TC, 7.18% in TG, 7.60% in LDL-C, and 14.06% increase in HDL-C, thereby restoring lipid parameters towards physiological levels (Figures. 1J-M).

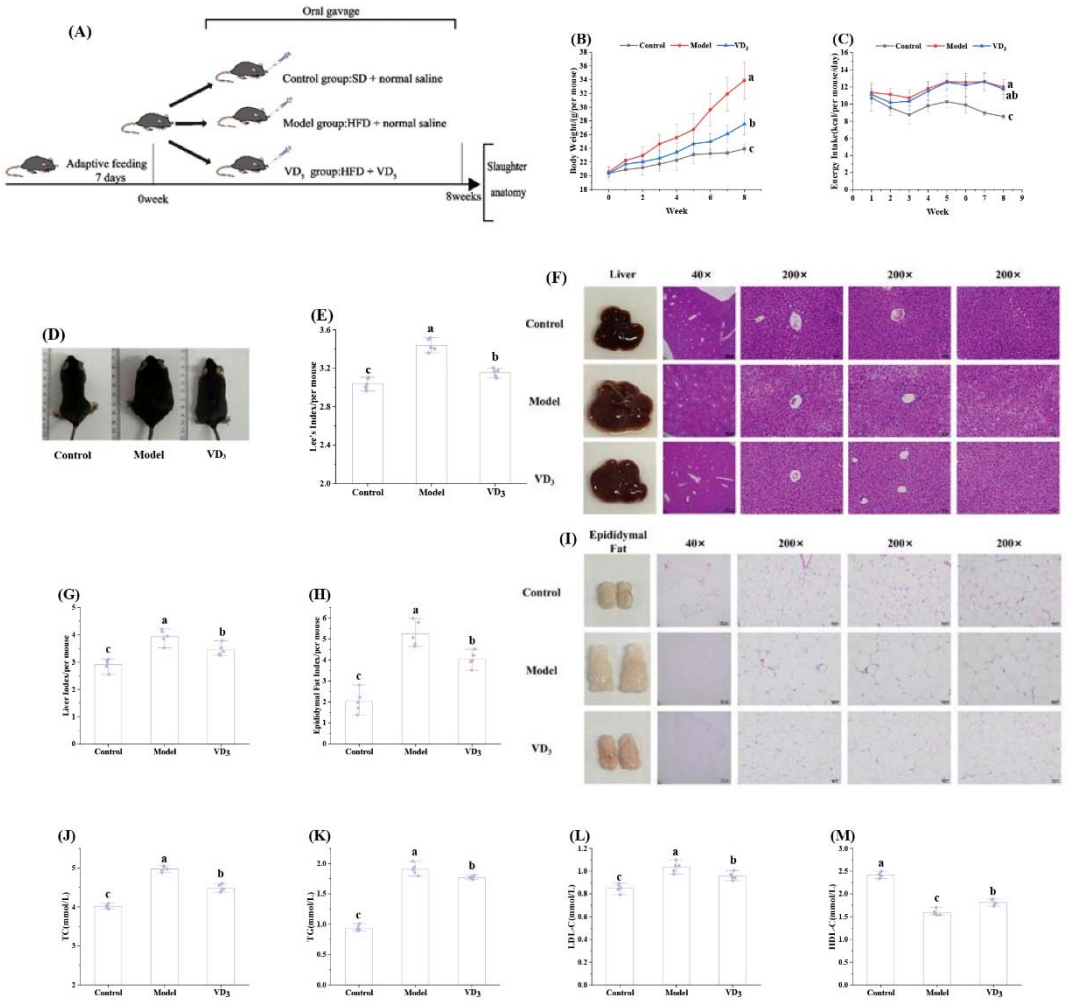

Figure 1. VD_3 supplementation has a lipid-lowering effect in HFD-fed mice. (A)Animal experiment arrangement. (B) Changes in body weight. (C) Changes in energy intake. (D) Representative photograph of mice. (E) The Lee's index. (F) Representative photograph and H&E staining with 40× and 200× magnification of liver tissue. (G) The liver index. (H) The epididymal fat index. (I) Representative photograph and H&E staining with 40× and 200× magnification of epididymal fat. (J) Serum TC. (K) Serum TG. (L) Serum LDL-C. (M) Serum HDL-C. a-c: bars with different letters indicate significant differences between groups (n=5 in each group, $P < 0.05$).

3.2 Effect of VD_3 supplementation on intestinal homeostasis in HFD-fed mice

3.2.1 Effect of VD_3 supplementation on intestinal health in HFD-fed mice

The intestinal tissues were removed from the -80 °C freezer, 9 times the volume of physiological saline was added. The mixture was mechanically homogenized under ice bath conditions to prepare a 10% homogenate. After centrifugation at 14000 ×g for 10 minutes, the supernatant from different intestinal tissues was collected and tested according to the kit instructions.

The redox status of the mouse intestine was assessed by measuring key biomarkers of lipid peroxidation (MDA) and antioxidant enzymes CAT and GSH-Px. The experimental results indicate that, the HFD-induced systemic oxidative stress, a key pathogenic mediator linking obesity to chronic inflammation, was significantly ameliorated by VD_3 supplementation through modulation of intestinal redox homeostasis. Oxidative damage assessment revealed that intestinal MDA levels, a key biomarker of lipid peroxidation, were significantly elevated in HFD-fed mice compared with the normal control group ($P < 0.05$). The most pronounced increases occurred in the ileum and colon, increased 407.50% and 132.99% respectively (Figure

2A-1). According to the results of the kit-based assays, VD_3 administration effectively attenuated this oxidative damage, reducing MDA levels by 38.42% in the ileum and 34.12% in the colon relative to the model group ($P < 0.05$). Antioxidant capacity analysis demonstrated that HFD feeding substantially compromised reductive enzyme activities. CAT activity was significantly decreased in the jejunum, ileum, and colon ($P < 0.05$) but showed no significant difference in the duodenum compared to controls. In contrast, GSH-Px activity was significantly reduced across all intestinal segments—duodenum, jejunum, ileum, and colon—in HFD-fed mice ($P < 0.05$). In the jejunum and colon, VD_3 intervention successfully restored intestinal antioxidant capacity, significantly increasing the activities of both CAT and GSH-Px. Specifically in the colon, compared with the control group, CAT and GSH-Px levels in the model group decreased by 36.34% and 32.60%, respectively. After VD_3 intervention, these levels recovered by 37.22% and 15.50%.

Obesity-induced chronic low-grade inflammation was modulated by VD_3 intervention. HFD feeding disrupted intestinal health, characterized by elevated pro-inflammatory cytokines, such as TNF-α, IL-6, and IL-1β, and suppressed anti-inflammatory cytokines (such as: IL-10) (Figure. 2B). As determined by ELISA, spatiotemporal analysis revealed segment-specific inflammatory responses: in ileum, HFD upregulated TNF-α, IL-6, and IL-1β by 108.33%, 41.02%, and 42.74%, respectively, compared with controls ($P < 0.05$). These increases were attenuated by VD_3 administration, which reduced them by 34.18%, 8.68%, and 11.92%, respectively ($P < 0.05$). Notably, IL-10 displayed inverse regulatory patterns: ileal IL-10 expression decreased by 40.81% in model mice($P < 0.05$), with VD_3 intervention showing a non-significant restorative trend ($P > 0.05$). In the colon, HFD-induced inflammation was more severe. Pro-inflammatory cytokines were markedly elevated: TNF-α by 135.75%, IL-6 by 64.14%, and IL-1β by 106.98% relative to controls ($P < 0.05$). VD_3 supplementation effectively mitigated these increases, reducing cytokine levels by 47.90%, 29.26%, and 33.69%, respectively ($P < 0.05$). In contrast to the ileum, VD_3 significantly counteracted HFD-induced suppression of IL-10 in the colon, increasing its expression by 17.12% compared to the model group ($P < 0.05$). Collectively, VD_3 demonstrated potent anti-inflammatory efficacy, particularly in the ileum and colon, through coordinated downregulation of pro-inflammatory cytokines and partial restoration of anti-inflammatory cytokines (Figure. 2B).

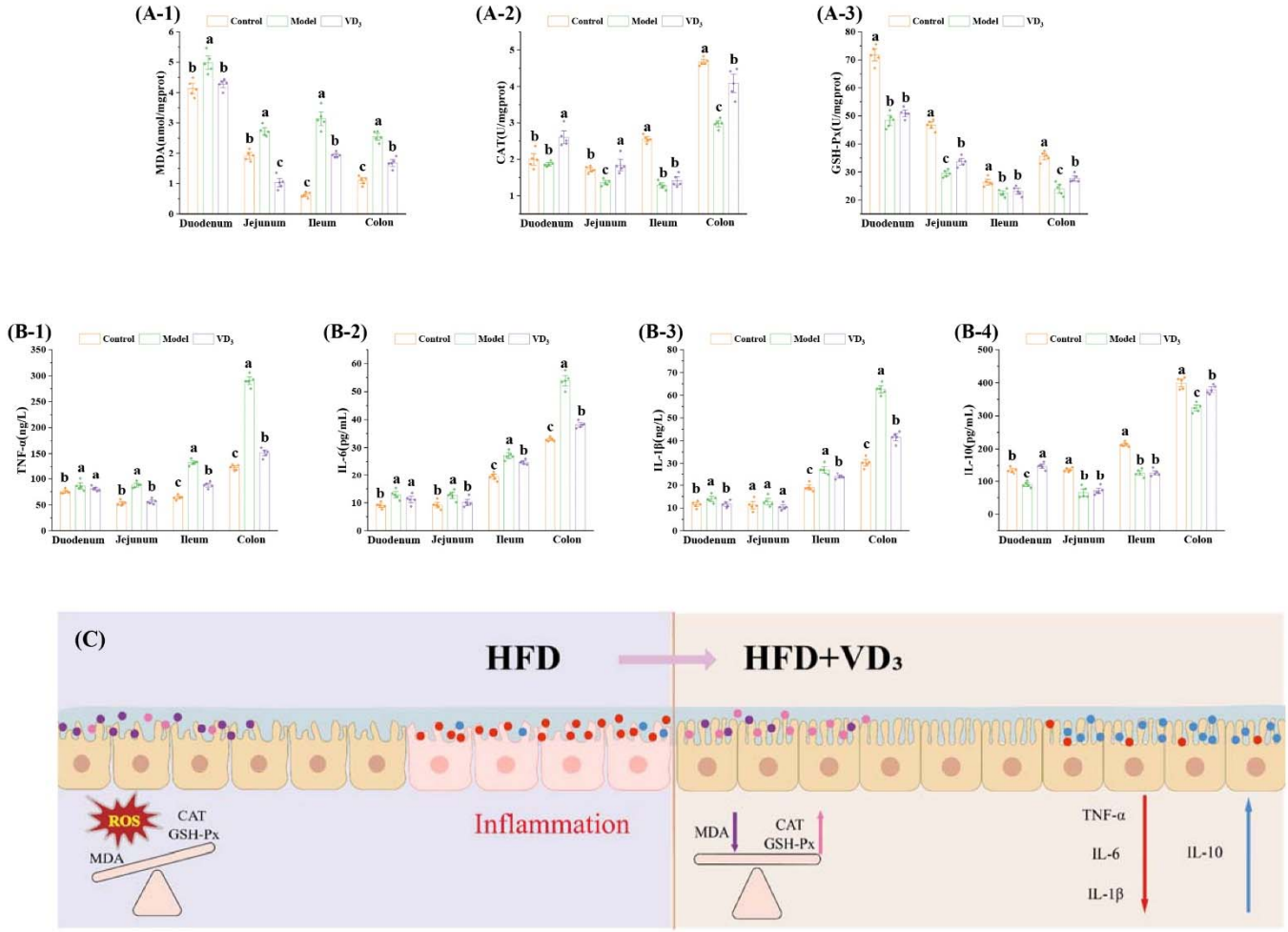

Figure 2. VD_3 supplementation alleviated intestinal oxidative stress and inflammation in HFD-fed mice. (A-1) MDA, (A-2) CAT, and (A-3) GSH-Px levels. (B-1) TNF-α, (B-2) IL-6, (B-3) IL-1β, and (B-4) IL-10 levels. (C) Schematic representation of the effects of VD_3 supplementation on intestinal oxidative stress and inflammation in HFD-fed mice. a-c: bars with different letters indicate significant differences between groups (n=5 in each group, $P < 0.05$).

3.2.2 Effect of VD_3 supplementation on the intestinal barrier in HFD-fed mice

The method for preparing intestinal tissue homogenate used in the kit is the same as above. As determined by ELISA, the HFD-induced intestinal barrier dysfunction was systematically mitigated by VD_3 through the coordinated restoration of physical, chemical, and immune barriers (Figure. 3). Histopathological evaluation demonstrated severe architectural disruption in model mice, showing villus rupture, severe atrophy, widened gland spacing, and marked colonic inflammatory infiltration. All of these changes were ameliorated by VD_3 (Figure. 3A). Serum D-lactate quantification (Figure. 3B), a biomarker of intestinal permeability, revealed a 18.85% elevation in model mice compared with the control group ($P < 0.05$). This increase was partially attenuated by VD_3 intervention, resulting in a 4.05% reduction ($P < 0.05$).

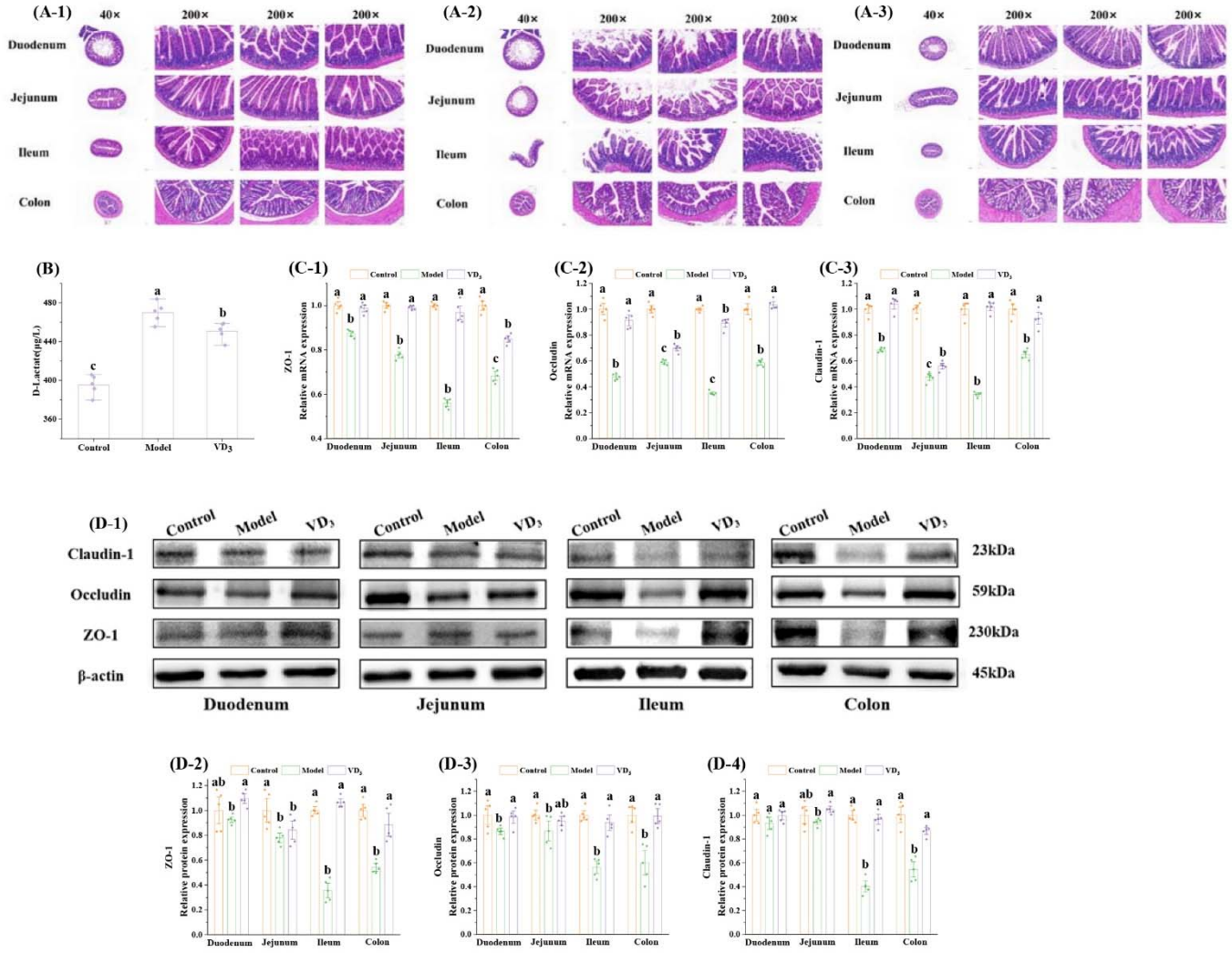

Figure 3. VD_3 supplementation improved the effect of the intestinal physical barrier in HFD-fed mice. H&E staining of different intestinal tissues in (A-1) control group, (A-2)model group and (A-3)VD_3 group mice with 40× and 200× magnification, (B) Serum D-lactate, (C-1) Z0-1, (C-2) Occludin, and (C-3) Claudin-1 relative mRNA expression, (D-1)Western blot bands, and (D-2) Z0-1, (D-3) Occludin, and (D-4) Claudin-1 relative protein expression. a-c: bars with different letters indicate significant differences between groups (n=5 in each group, $P < 0.05$).

The 50-100 mg of intestinal tissues were removed from the -80 °C freezer. 1 mL of lysis buffer and two sterile steel beads were added. The mixture was mechanically homogenized under ice bath conditions to prepare a 10% homogenate. After centrifugation, the supernatant from different intestinal tissues was collected for subsequent qPCR testing.

qPCR and Western blot analysis of TJ proteins revealed segment-specific dysregulation. In the model mice, the mRNA expressions of three TJ proteins (Figures. 3C) were significantly reduced across all four intestinal segments compared to the normal control groups ($P < 0.05$), with the most pronounced decrease observed in the ileum. In the ileum, ZO-1, Occludin, and Claudin-1 mRNA expressions dropped by 44.12%, 64.87%, and 65.87%, respectively ($P < 0.05$). Further Western blot analysis (Figures. 3D) revealed that HFD significantly reduced the protein expression levels of intestinal TJ proteins in mice, particularly in the ileum and colon. Compared with the control group, the protein expression of ZO-1, Occludin, and Claudin-1 in the ileum decreased by 64.51%, 43.81%, and 59.82%, respectively ($P < 0.05$). Similarly, in the colon, the protein expression level of ZO-1, Occludin, and Claudin-1 were reduced by 45.78%, 40.01%, and 45.72%,

respectively ($P < 0.05$), VD_3 treatment restored TJ proteins expression to control levels, with maximal efficacy observed in the ileum (Figures. 3C, D). As determined by ELISA, the intestinal chemical barrier, primarily constituted by MUC2 and REG3γ, exhibited segment-specific vulnerability to HFD-induced damage (Figure. 4). Compared with controls, HFD-induced model mice showed reduced goblet cells (Figures. 4A, B-1) and MUC2 expression (Figure. 4B-2) across intestinal segments. VD_3 intervention significantly increased MUC2 expression by 25.66% in the duodenum and 8.68% in the ileum ($P < 0.05$), whereas no significant changes were observed in the jejunum or colon ($P > 0.05$). Compared with the control group, the expressions of REG3γ (Figure. 4B-3) were significantly reduced in all four intestinal segments in the model group ($P < 0.05$). The effect of VD_3 on REG3γ displayed distinct spatial regulation patterns: while no significant change was observed in the jejunum ($P > 0.05$), the most pronounced increase occurred in the ileum and colon. In the ileum, model mice exhibited a 41.09% decrease, which was nearly reversed by VD_3 treatment ($P < 0.05$). Colonic expression suffered severe depletion of 65.11%, which was rescued to control levels through a 1.1-fold upregulation mediated by VD_3.

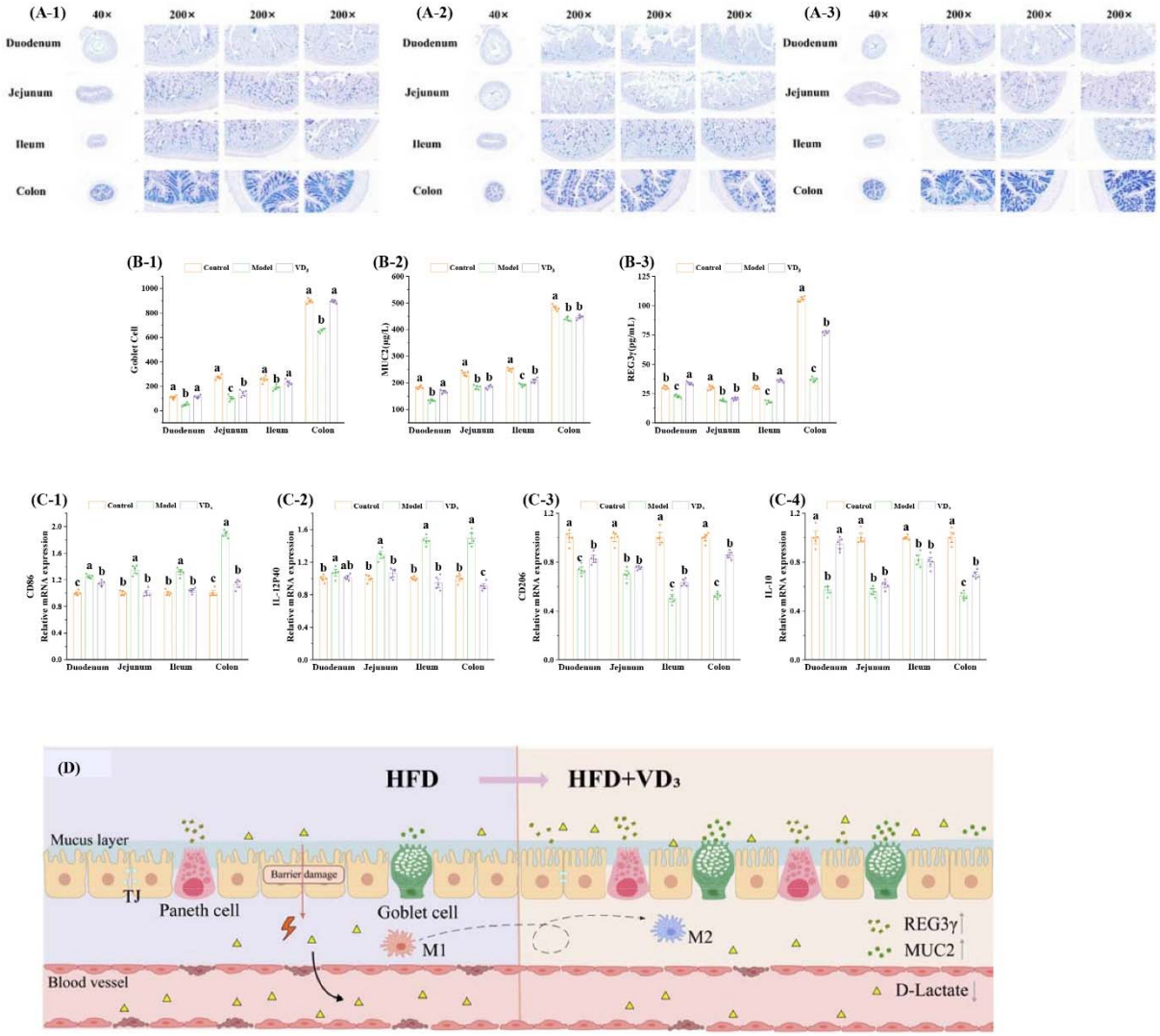

Figure 4. VD_3 supplementation improved the effect of the intestinal barrier in HFD-fed mice. AB-PAS staining of different intestinal tissues in (A-1) control group, (A-2)model group and (A-3)VD_3 group mice with 40× and 200× magnification, staining of the different intestinal sections with 200× magnification, (B-1) the number of goblet cells, (B-2) MUC2, and (B-3) REG3γ levels. (C-1) CD86, (C-2) IL-12P40, (C-3) CD206, and (C-4) IL-10 relative mRNA expression. (D) Schematic representation of the effect of VD_3 supplementation on intestinal homeostasis in HFD-fed mice. a-c: bars with different letters indicate significant differences between groups (n=5 in each group, $P < 0.05$).

The method for preparing intestinal tissue homogenate used in the qPCR is the same as above. Immunophenotypic profiling via qPCR revealed HFD-induced macrophage polarization imbalance (Figure. 4C). In the model group, compared with controls, M1 macrophage markers CD86 and IL-12P40 exhibited colonic predominance (upregulated by 88.75% and 49.10%, respectively ($P < 0.05$)), contrasting with suppressed M2 macrophage markers (CD206 and IL-10 downregulated by 47.25% and 47.73%, respectively($P < 0.05$)). VD_3 supplementation rebalanced intestinal immune homeostasis, indicating VD_3-mediated immune barrier fortification through macrophage functional reprogramming.

3.3 Effect of VD3 supplementation on the composition and structure of the gut microbiota in HFD-fed mice

Mice were dissected in a biosafety cabinet and different **intestinal** tissue samples were collected from each group of mice for gut microbiota testing.

Building on the spatial susceptibility of ileocolonic segments to HFD-induced metabolic perturbation (Figures. 2-4)**,** we conducted targeted microbiota profiling to elucidate VD_3's modulatory effects (Figures. 5-7). 16S rRNA gene sequencing revealed significant microbial community restructuring in model mice. The Chao1 index and Shannon index (Figure. 5A) indicated lower microbial diversity, and principal coordinate analysis (PCoA) (Figure. 5B) showed a distinct flora structure in the model group compared to the control group. Venn diagrams displayed differences in Operational Taxonomic Units (OTU) among the three groups (Figure. 5C). Linear discriminant analysis (LEfSe) (Figure. 5D) and heatmap (Figure. 5E) demonstrated that, compared to the control group, the dominant bacteria in the model group shifted from *Lactobacillus* and *Odoribacter* to *Faecalibaculum* and *Romboutsia*. VD_3 intervention restored microbial diversity to levels similar to controls and normalized the heatmap clustering patterns (Figure. 5E).

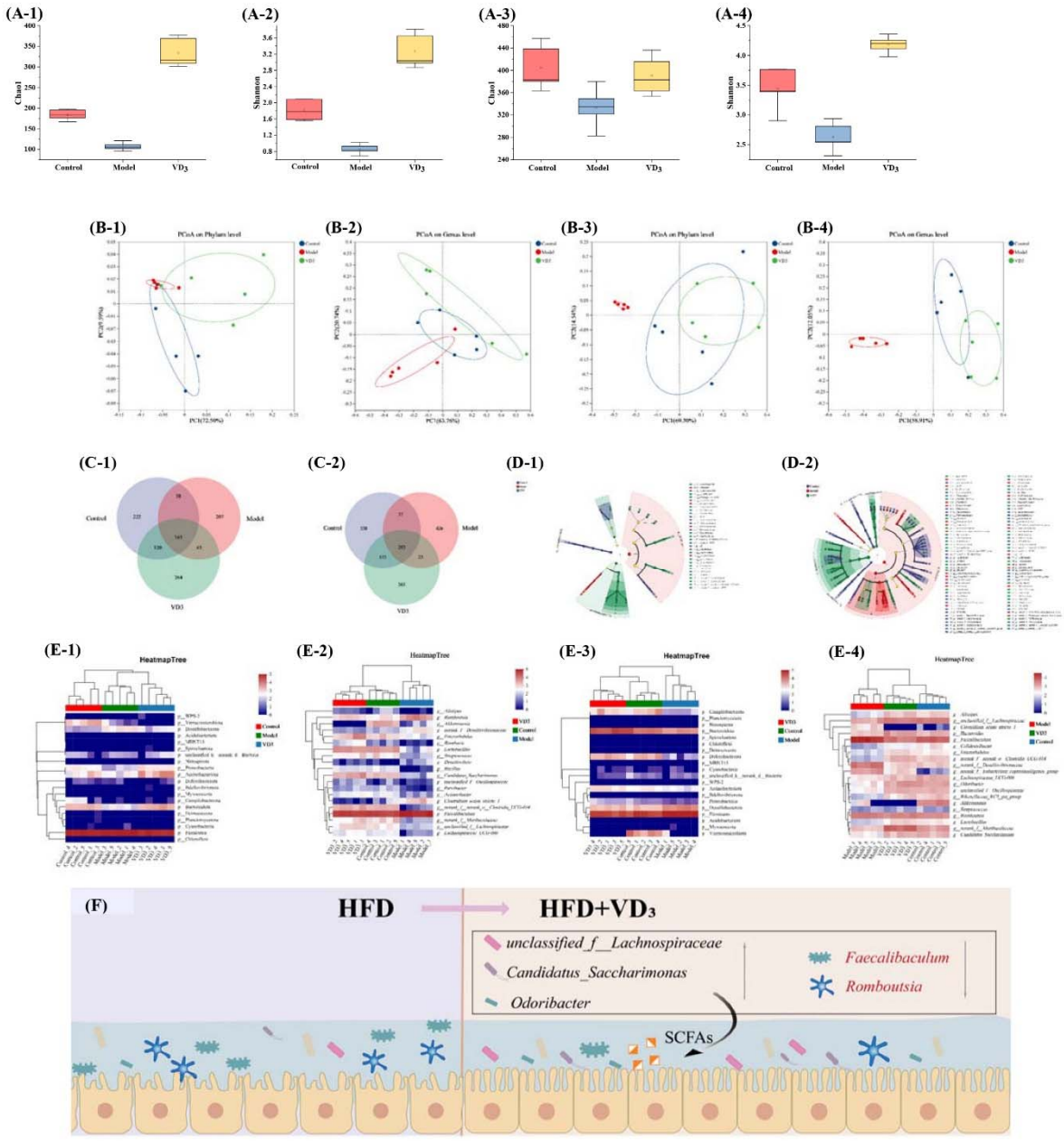

Figure 5. VD_3 supplementation restored intestinal microbiota diversity in HFD-fed mice. (A-1) Chao1 and (A-2) Shannon index in ileum. (A-3) Chao1 and (A-4) Shannon index in colon. (B-1) PCoA at the phylum and (B-2) genus levels in ileum. (B-3) PCoA at the phylum and (B-4) genus levels in colon. (C-1) Venn diagrams on the OUT level in ileum and (C-2) colon. (D-1) LEfSe evolutionary branch diagram in ileum and (D-2) colon. (E-1) Heatmap of the top 20 gut microbiota for each group at the phylum and (E-2) genus levels in ileum. (E-3) Heatmap of the top 20 gut microbiota for each group at the phylum and (E-4) genus levels in colon. (F) Schematic representation of the effects of VD_3 supplementation on gut flora abundance in HFD-fed mice. a-c: bars with different letters indicate significant differences between groups (n=5 in each group, $P < 0.05$).

We analyzed how VD_3 affects gut microbiota in HFD-fed mice furtherly. Phylum-level stratification demonstrated that HFD induced an amplification of the Firmicutes/Bacteroidota (F/B) ratio in both ileum and colon. However, VD_3 alleviated this effect. Notably, compared to the control group, colonic Firmicutes in HFD-fed mice surged from 39.62% to 87.58% ($P < 0.05$), correlating with pro-inflammatory markers. This suggests more severe colon inflammation and highlights the need for obesity regulation focus in this area (Figures. 6-7). Genus-level resolution revealed spatial intervention specificity. In the ileum, control mice had dominant *Faecalibaculum* (42.45%) (Figure. 6B-2), *Romboutsia* (0.86%) (Figure. 6B-3) and *Lactobacillus*

(3.77%) (Figure. 6B-4), which became 80.40%, 6.81%, and 0.75% in the model group. In the colon, harmful *Faecalibaculum* (Figure. 7B-2) and *Romboutsia* (Figure. 7B-3) increased from 19.63% and 6.79% in the control group to 58.79% and 9.41% in the model group ($P < 0.05$). Yet, VD_3 reduced them to 7.57% and 7.18%, respectively ($P < 0.05$). Beneficial bacteria such as *Lachnospiraceae* (Figure. 7B-4), *Odoribacter*, (Figure. 7B-5) and *Candidatus_Saccharimonas* (Figure. 7B-6) decreased in the model group but were restored by VD_3 from. However, *Akkermansia*'s relative abundance fell in the model group and did not recover with VD_3 ($P > 0.05$) (Figures. 6B-4, 7B-7).

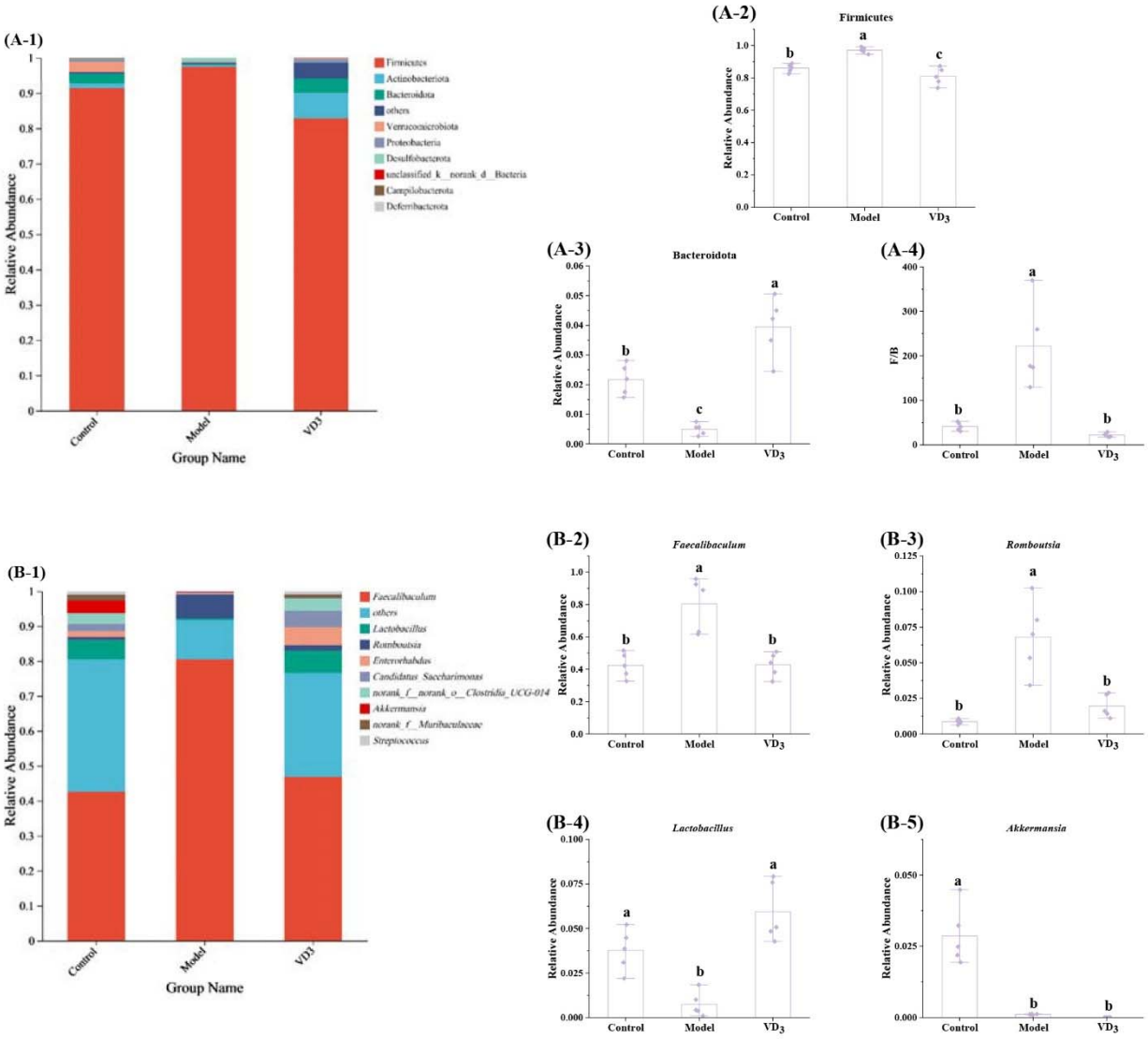

Figure 6. VD_3 modulates the composition of the ileal gut microbiota in HFD-fed mice. (A-1) Changes in gut microbiota at the phylum level in ileum. (A-2) Relative abundances of Firmicutes and (A-3) Bacteroidota. (A-4) F/B ratio. (B-1) Changes in gut microbiota at the genus level in ileum. (B-2) Relative abundances of *Faecalibaculum*, (B-3) *Romboutsia*，(B-4) *Lactobacillus* and (B-5) *Akkermansia*. a-c: bars with different letters indicate significant differences between groups (n=5 in each group, $P < 0.05$).

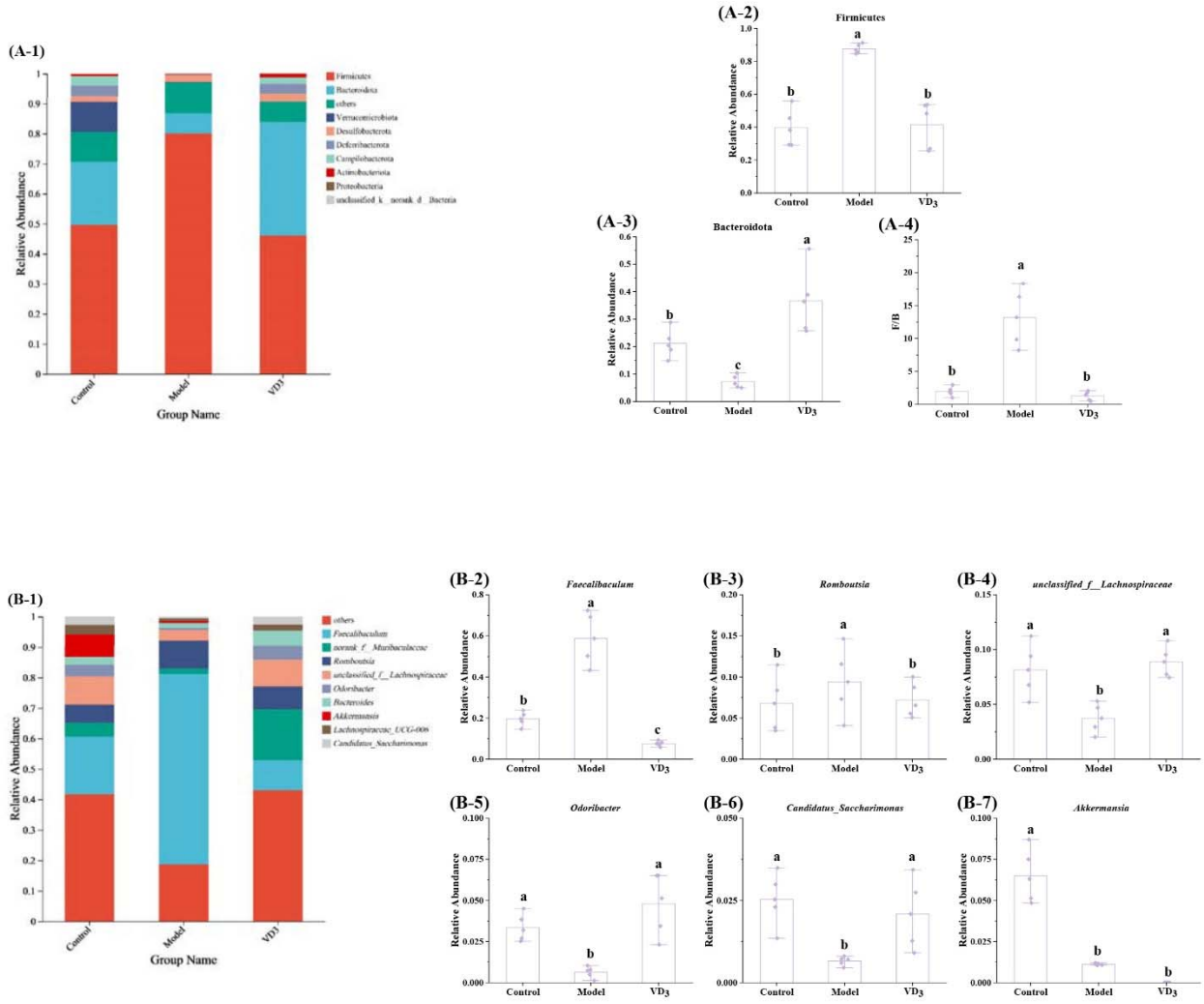

Figure 7. VD_3 modulates the composition of the colonic gut microbiota in HFD-fed mice. (A-1) Changes in gut microbiota at the phylum level in colon. (A-2) Relative abundances of Firmicutes and (A-3) Bacteroidota. (A-4) F/B ratio. (B-1) Changes in gut microbiota at the genus level in colon. (B-2) Relative abundances of *Faecalibaculum*, (B-3) *Romboutsia*, (B-4) *unclassified_f__Lachnospiraceae*, (B-5) *Odoribacter*, (B-6) *Candidatus_Saccharimonas*, and (B-7) *Akkermansia*. a-c: bars with different letters indicate significant differences between groups (n=5 in each group, $P < 0.05$).

4. Discussion

Over the past few years, the intricate relationship between obesity and intestinal homeostasis has garnered significant attention from the scientific community. In our study, we investigated the interplay between VD_3 and intestinal homeostasis imbalance in HFD-fed mice. By analyzing the regulatory effects of VD_3 on different intestinal segments, we aimed to uncover the targeted regulatory mechanisms through which VD_3 influences intestinal homeostasis, thereby providing novel insights into the complex pathophysiology of obesity-related intestinal dysfunction.

This study systematically investigated the regulatory effects of VD_3 on intestinal homeostasis in male C57BL/6J mice maintained on an HFD for 8 weeks. Experimental data showed that HFD feeding causes intracellular lipid deposition in intestinal epithelial cells. This lipid deposition promotes the production of reactive oxygen species (ROS) and increases the metabolic burden of the intestine[24]. This lipotoxic microenvironment precipitated structural disintegration of epithelial cells, initiated oxidative stress cascades,

and impaired barrier integrity[25]. Subsequently, these pathological alterations induced disrupted the immune system and upset gut balance. Consistent with previous studies, HFD has been shown to induce oxidative stress in mice, compromise their antioxidant capacity, and thereby impair intestinal health[26]. Our findings demonstrated that HFD exposure overwhelmed antioxidant defensive system, creating a pro-oxidative state that disrupted intestinal homeostasis. As a marker of oxidative stress, the elevation of MDA activity is associated with obesity and its comorbidities, while concurrent depletion of CAT and GSH-Px activities confirmed systemic antioxidant depletion[10]. However, VD_3 supplementation remarkably bolstered the antioxidant capacity of the intestines in HFD-fed mice, protected gut tissue from lipid peroxidation, and mitigated oxidative stress and intestinal homeostasis disorder. Spatial analysis revealed segment-specific therapeutic efficacy, with the ileum and colon demonstrating greater susceptibility to oxidative damage and correspondingly enhanced responsiveness to VD_3 treatment. The persistent oxidative burden activated pro-inflammatory pathways, damaged intestinal epithelial cells[24], caused mucosal barrier and immune system destruction[25], leading to an imbalance of pro-inflammatory cytokines and intestinal inflammation. These findings underscore the regional vulnerability of distal intestinal segments to HFD-induced inflammatory pathogenesis.

To validate our hypothesis, we systematically measured pro-inflammatory factors across 4 distinct intestinal regions (duodenum, jejunum, ileum and colon) in mice. TNF-α, a key inflammatory marker, exhibited elevated levels in the model group, effectively reflects inflammation severity[27]. Consistently, IL-6 and IL-1β levels rose in the model group, while IL-10 level fell, indicating inflammation throughout all intestinal segments, with the most severe effects observed in the ileum and colon. These observations validated our hypothesis of region-specific inflammatory susceptibility. Crucially, VD_3 intervention demonstrated significant anti-inflammatory efficacy, normalizing inflammatory factors and restoring immune equilibrium, thereby substantiating its protective role in maintaining intestinal homeostasis under obesogenic stress.

The synergistic effects of oxidative stress and chronic inflammation induce multifaceted damage to intestinal barrier components, including structural compromise of epithelial cells, functional impairment of mucin-secreting goblet cells, dysregulation of antimicrobial Paneth cells, and altered immunomodulatory capacity of intestinal macrophages[28]. Obesity-associated metabolic dysregulation was corroborated by elevated serum D-lactate level, a biomarker indicative of paracellular permeability[29]. VD_3 intervention effectively restored barrier integrity, significantly attenuating HFD-induced hyperpermeability through dual mechanisms: 1) Preserving the structural integrity of villus architecture, which is critical for nutrient absorption and barrier maintenance, and 2) Regulating TJ proteins. Histological analysis confirmed VD_3-mediated mitigation of HFD-induced villus blunting. At the molecular level, TJ proteins constitute essential structural components of the intestinal physical barrier, maintaining epithelial continuity through precise regulation of paracellular transport pathways[30]. HFD-induced obesity disrupted TJ proteins homeostasis, particularly affecting ZO-1, Occludin, and Claudin-1 expressions, thereby exacerbating

paracellular leakage[31]. VD_3 administration counteracted this pathology by upregulating mRNA and protein expression of these TJ proteins, reinforcing epithelial continuity. These findings collectively demonstrate that VD_3 preserves intestinal homeostasis in HFD-fed mice through structural stabilization of the physical barrier and molecular restoration of TJ proteins.

The intestinal chemical barrier, composed of mucus secretions and antimicrobial effectors, plays a pivotal role in maintaining mucosal homeostasis. Goblet cell-derived mucus forms a selectively permeable interface that shields the epithelium from harmful substances, a protective mechanism compromised in HFD-fed mice through significant goblet cell depletion, which was ameliorated by VD_3 supplementation[32]. Central to this barrier, MUC2 constitutes the structural backbone of the mucus layer, preventing direct microbial-epithelial contact[33], while REG3γ, an antibacterial substance, maintains intestinal microflora balance by reducing harmful bacteria[34]. HFD feeding suppressed both MUC2 biosynthesis and REG3γ expression, likely due to losses of mucus-producing goblet cells and antimicrobial peptide-secreting Paneth cells[35]. VD_3 intervention increased MUC2 and REG3γ levels, which counteracted these deficits, restoring mucus layer integrity and antimicrobial activity, thereby reinforcing epithelial defensive mechanisms[36]. Although these protective effects were observed throughout the intestinal tract, ileal segments exhibited the most pronounced VD_3-mediated recovery, highlighting both the region-specific vulnerability of the ileum to HFD-induced chemical barrier disruption and its heightened responsiveness to VD_3-driven mucosal rehabilitation. These findings underscore VD_3's capacity to restore HFD-induced chemical barrier function, with particular efficacy in ileum.

Emerging evidence highlights the critical role of macrophage polarization in intestinal homeostasis, with oxidative stress and inflammation directly modulating phenotypic transitions between M1 and M2 macrophage subsets[37-38]. To assess VD_3's immunomodulatory effects, we analyzed intestinal mRNA expression of polarization markers: M1-associated CD86 and IL-12P40, and M2-associated CD206 and IL-10. HFD-induced oxidative-inflammatory stress skewed macrophages toward the pro-inflammatory M1 phenotype, marked by upregulated CD86 and IL-12P40 alongside suppressed CD206 and IL-10 expressions, perpetuating intestinal damage through sustained pro-inflammatory cytokines and ROS release[7, 39]. VD_3 supplementation appeared to reverse this imbalance, downregulating M1 markers while enhancing M2 signature expression, suggesting a shift in macrophage polarization toward anti-inflammatory phenotypes. This reprogramming was correlated with restored IL-10-mediated immunoregulation and attenuated inflammatory cascades, indicating VD_3's potential capacity to mitigate oxidative stress–inflammation crosstalk through macrophage phenotypic modulation[7, 39]. By potentially rebalancing immune effector functions, VD_3 may alleviate intestinal barrier deterioration and help maintain intestinal homeostasis, underscoring its therapeutic potential in restoring immune barrier integrity under HFD feeding. However, it is important to note that the M1/M2 polarization framework, while widely used, requires further direct experimental validation in this specific context. The evidence currently supporting the shift in macrophage

polarization is largely based on marker expression, and more further supporting evidence would be necessary to definitively establish VD_3's role in modulating macrophage phenotypes.

In summary, HFD-induced tripartite barrier dysfunction involving physical disruption (tight junctional integrity), chemical depletion (mucus layer attenuation), and immune dysregulation (macrophage polarization imbalance) across murine intestinal segments, linked to oxidative-inflammatory axis activation. VD_3 intervention counteracts these pathological cascades by coordinately restoring epithelial junctional integrity, mucus biosynthesis, and anti-inflammatory macrophage polarization, thereby reestablishing intestinal homeostasis. Notably, the distal intestinal segments (ileum/colon) exhibit heightened susceptibility to barrier damage, aligning with their greater susceptibility to oxidative stress and inflammation.

The ileum, as the primary segment for nutrient absorption, requires a finely-tuned immune system to maintain a balance between tolerance and defense. The significant responsiveness to VD_3 regulation we observed in the ileum aligns with its role in promoting epithelial integrity and modulating immune responses, thereby supporting its absorptive function while preventing inflammation. In contrast, the colon serves as a habitat for a vast and diverse microbial community, with its physiological state centered on microbial colonization and minimal involvement in nutrient absorption. Here, the action of VD_3 is likely integrated with microbiota-derived signals to collectively maintain local gut homeostasis. These inherent physiological differences underlie the remarkable "spatial specificity" observed in VD_3 regulation.

Dysbiosis of the gut microbiota represents a well-established etiological factor in intestinal homeostasis disruption, mediated through multifaceted regulatory mechanisms including modulation of short-chain fatty acids (SCFAs) biosynthesis—particularly butyrate—and dynamic control of inflammatory factors[7, 9, 12]. To elucidate VD_3's microbiota-targeted regulatory role, we conducted 16S rRNA sequencing analysis of ileal and colonic communities in HFD-fed mice. Analytical results demonstrated that VD_3 administration restructured the gut microbiota composition and structure in HFD-fed mice, effectively reestablishing microbial equilibrium and promoting intestinal homeostasis through targeted modulation of core commensal communities.

The experimental findings demonstrated that VD_3 intervention significantly modulated the gut microbial composition, with particular phylum-level alterations. Notably, the model group exhibited a marked increase in Firmicutes abundance accompanied by reduced Bacteroidetes. This change associated with pro-inflammatory responses through elevated TNF-α production [27], particularly in the colon. The resultant Firmicutes/Bacteroidetes (F/B) ratio elevation observed in both ileal and colonic segments of model group align with established biomarkers of intestinal dysbiosis[15]. Supplementation with VD_3 effectively normalized this ratio through targeted microbial modulation. Although our study confirms the strong correlation between an elevated F/B ratio and inflammation, the mechanism by which VD_3 normalizes this ratio remains an open question. It is plausible that the restoration of the F/B ratio may be a consequence of VD_3 improving the intestinal barrier and reducing inflammation, thereby creating a habitat that is less favorable for pro-inflammatory Firmicutes and more conducive to beneficial Bacteroidetes.

Further analysis indicated distinct regional variations in bacterial abundance. Colonic microbiota showing more pronounced Firmicutes proliferation and corresponding TNF-α level elevation, compared to ileal samples, suggesting heightened susceptibility of colonic microenvironments to HFD-induced inflammatory pathways.

VD_3 supplementation exerted genus-specific modulatory effects on intestinal microbiota in HFD-fed mice. Specifically, it significantly restored the abundance of *Lactobacillus*, a commensal probiotic genus critically involved in intestinal barrier maintenance. *Lactobacillus* contributes to barrier maintenance through transcriptional regulation of MUC2 and TJ proteins[12, 40]. The precise reason for the selective restoration of *Lactobacillus* by VD_3 is intriguing. Since we also observed VD_3-mediated upregulation of REG3γ and MUC2, it is possible that the antimicrobial activity of REG3γ cleared niche competitors, thereby favoring *Lactobacillus* colonization. In the ileal microbiota of model mice, *Lactobacillus* displayed marked depletion but recovered following VD_3 intervention, suggesting a plausible mechanism for VD_3 in preserving ileal homeostasis. Concomitantly, HFD-induced dysbiosis manifested through ileocolonic proliferation of pro-inflammatory genera including *Faecalibaculum* (associated with exacerbation of intestinal inflammation and metabolic disturbances[41]) and *Romboutsia* (implicated in TLR4-mediated activation of inflammatory signaling cascades that compromise epithelial barrier integrity[36, 42]), both of which were effectively suppressed by VD_3 treatment. Notably, VD_3 ameliorated these microbial imbalances while concurrently restoring colonic abundances of SCFAs-producing taxa such as *Lachnospiraceae*, *Candidatus_Saccharimonas*, and *Odoribacter*[15, 41], which were diminished in model mice. Their restoration potentially enhancing epithelial barrier integrity through SCFAs-mediated mechanisms including butyrate-dependent stimulation of TJ proteins biosynthesis[12, 15, 36, 41]. These coordinated modulations of microbial consortia substantiate VD_3's therapeutic potential in counteracting HFD-induced intestinal dysfunction through microbiota-targeted pathways.

This targeted restructuring rebalances core commensal populations critical for butyrogenic metabolism and anti-inflammatory signaling, thereby ameliorating HFD-induced dysbiosis. The observed microbial restoration substantiated VD_3's capacity to rectify microbiota-host crosstalk in obesogenic contexts. Notably, the ileocolonic axis, a pivotal site for microbial interaction, emerged as the primary focus of VD_3-mediated microbial rehabilitation. These findings position VD_3 as a potent modulator of HFD-induced microbial ecology perturbations, operating through region-specific microbiota reprogramming to reinstate intestinal homeostasis.

Furthermore, it is important to acknowledge the limitations of this study. First, the study lacked a VD_3 concentration gradient; while the selected 15,000 IU/kg gavage dose was literature-supported for safety and efficacy in modulating obesity-related phenotypes, the single-dose design prevented characterizing a dose-response relationship. Second, only male mice were used, failing to consider gender differences in VD_3 metabolism and gut homeostasis, which may limit the generalization of findings. Third, the 8-week intervention period was relatively short, with no observation of VD_3's long-term effects on obesity recurrence

and gut homeostasis stability. Fourth, though VD_3's regulatory effect on gut microbiota was observed, specific molecular pathways (e.g., whether mediated by vitamin D receptor VDR) were not further verified. Fifth, while the observed effects were statistically strong and consistent, the limited sample size (n=5 per group) may affect the statistical power of the analysis, particularly for detecting smaller effects. Future studies with larger cohort sizes will address these by setting VD_3 concentration gradients, including both male and female animals, designing long-term interventions, and conducting targeted experiments to clarify underlying mechanisms, thus providing more comprehensive evidence for VD_3's role in regulating gut homeostasis.

5. Conclusions

In conclusion, VD_3 restores intestinal homeostasis in HFD-fed mice through two synergistic mechanisms: mitigating oxidative stress and inflammation, and modulating gut microbiota composition and function. These effects exhibit distinct segment-specificity, with the ileum showing pronounced improvement in barrier proteins (TJ proteins, MUC2) and *Lactobacillus* abundance, while the colon displayed stronger immunoregulatory effects on macrophage polarization and inflammation, coupled with enrichment of *Lachnospiraceae*. Our findings underscore the potential of VD_3 as a targeted nutritional strategy for segment-specific interventions in intestinal diseases.

Conflicts of interest

The authors declare no conflict of interest.

Acknowledgement

This research was funded by National Key Research and Development Program of China (grant number 2022YFF1100102-5).

References

[1] J. Sun, Y. Zhang, Vitamin D receptor influences intestinal barriers in health and disease, Cells-Basel. 11 (2022) 1129. https://doi.org/10.3390/cells11071129.

[2] M. Song, S. Zhang, Z. Tao, et al., MMP-12 siRNA improves the homeostasis of the small intestine and metabolic dysfunction in high-fat diet feeding-induced obese mice, Biomaterials. 278 (2021) 121183. https://doi.org/10.1016/j.biomaterials.2021.121183.

[3] Y. Wan, B. Zhang, The impact of zinc and zinc homeostasis on the intestinal mucosal barrier and intestinal diseases, Biomolecules. 12 (2022) 900. https://doi.org/10.3390/biom12070900.

[4] S. Riedel, C. Pheiffer, R. Johnson, et al., Intestinal barrier function and immune homeostasis are missing links in obesity and type 2 diabetes development, Front Endocrinol. 12 (2022) 833544-833544. https://doi.org/10.3389/fendo.2021.833544.

[5] A. Toubal, B. Kiaf, L. Beaudoin, et al., Mucosal-associated invariant T cells promote inflammation and intestinal dysbiosis leading to metabolic dysfunction during obesity, Nat Commun. 11 (2020). https://doi.org/10.1038/s41467-020-17307-0.

[6] Y.C. Chooi, C. Ding, F. Magkos, The epidemiology of obesity, Metabolism. 92 (2019) 6-10. https://doi.org/10.1016/j.metabol.2018.09.005.

[7] Y. Belkaid, O.J. Harrison, Homeostatic immunity and the microbiota, Immunity. 46 (2017) 562-576. https://doi.org/10.1016/j.immuni.2017.04.008.

[8] M. Blüher, M. Aras, L.J. Aronne, et al., New insights into the treatment of obesity, Diabetes Obes Metab. 25 (2023) 2058-2072. https://doi.org/10.1111/dom.15077.

[9] Y. Fu, Q. Wang, Z. Tang, et al., Cordycepin ameliorates high fat diet-induced obesity by modulating endogenous metabolism and gut microbiota dysbiosis, Nutrients. 16 (2024) 2859. https://doi.org/10.3390/nu16172859.

[10] S. Khateeb, A. Albalawi, A. Alkhedaide, Diosgenin modulates oxidative stress and inflammation in high-fat diet-induced obesity in mice, Diabet Metab Synd Ob. 15 (2022) 1589-1596. https://doi.org/10.2147/DMSO.S355677.

[11] S. Patil, M. Das, G.S. Kumar, et al., Coffee leaf extract exhibits anti-obesity property and improves lipid metabolism in high-fat diet-induced C57BL6 obese mice, 3 Biotech. 13 (2023) 278. https://doi.org/10.1007/s13205-023-03698-6

[12] Y. Ma, H. Xie, N. Xu, et al., Large yellow tea polysaccharide alleviates HFD-induced intestinal homeostasis dysbiosis via modulating gut barrier integrity, immune responses, and the gut microbiome, J Agr Food Chem. 72 (2024) 7230-7243. https://doi.org/10.1021/acs.jafc.4c00616.

[13] C.Y. Park, Y. Shin, J. Kim, et al., Effects of high fat diet-induced obesity on vitamin D metabolism and tissue distribution in vitamin D deficient or supplemented mice, Nutr Metab. 17 (2020) 44. https://doi.org/10.1186/s12986-020-00463-x.

[14] C.Y. Park, T.Y. Kim, J.S. Yoo, et al., Effects of 1,25-dihydroxyvitamin D_3 on the inflammatory responses of stromal vascular cells and adipocytes from lean and obese mice, Nutrients. 12 (2020) 364. https://doi.org/10.3390/nu12020364.

[15] L. Xiang, T. Du, J. Zhang, et al., Vitamin D_3 supplementation shapes the composition of gut microbiota and improves some obesity parameters induced by high-fat diet in mice, Eur J Nutr. 63 (2024) 155-172. https://doi.org/10.1007/s00394-023-03246-1.

[16] H.M.A. Fakhoury, P.R. Kvietys, W. AlKattan, et al., Vitamin D and intestinal homeostasis: Barrier, microbiota, and immune modulation, J Steroid Biochem. 200 (2020) 105663. https://doi.org/10.1016/j.jsbmb.2020.105663.

[17] B. Alzohily, A. AlMenhali, S. Gariballa, et al., Unraveling the complex interplay between obesity and vitamin D metabolism, Sci Rep-Uk. 14 (2024). https://doi.org/10.1038/s41598-024-58154-z.

[18] A. Marziou, C. Philouze, C. Couturier, et al., Vitamin D supplementation improves adipose tissue inflammation and reduces hepatic steatosis in obese C57BL/6J mice, Nutrients. 12 (2020) 342. https://doi.org/10.3390/nu12020342.

[19] S.J. Kim, D.H. Cho, G.Y. Lee, et al., The effects of dietary vitamin D supplementation and in vitro 1,25 dihydroxyvitamin D_3 treatment on autophagy in bone marrow-derived dendritic cells from high-fat diet-induced obese mice, Nutr Biochem. 100 (2022) 108880. https://doi.org/10.1016/j.jnutbio.2021.108880.

[20] J. Zhang, Y. Zhang, Y. Zhou, et al., Effect of vitamin D_3 on lipid droplet growth in adipocytes of mice with HFD-induced obesity, Food Sci Nutr. 11 (2023) 6686-6697. https://doi.org/10.1002/fsn3.3618.

[21] M. Furuhashi, G.S. Hotamisligil, Fatty acid-binding proteins: role in metabolic diseases and potential as drug targets, Nat Rev Drug Discov. 7 (2008) 489-503. https://doi.org/10.1038/nrd2589.

[22] R. Chen, L. Xu, S. Du, et al., *Lactobacillus* rhamnosus GG supernatant promotes intestinal barrier function, balances T reg and T H 17 cells and ameliorates hepatic injury in a mouse model of chronic-binge alcohol feeding, Toxicol Lett. 241 (2016) 103-110. https://doi.org/10.1016/j.toxlet.2015.11.019.

[23] Y. Lee, K. Sugihara, M.G. Gillilland, et al., Hyaluronic acid–bilirubin nanomedicine for targeted modulation of dysregulated intestinal barrier, microbiome and immune responses in colitis, Nat Mater. 19 (2020) 118-126. https://doi.org/10.1038/s41563-019-0462-9.

[24] O.C. Edward, S.S. Thomas, K. Cha, et al., Green perilla leaf extract ameliorates long-term oxidative stress induced by a high-fat diet in aging mice, Nutr Res Pract. 16 (2022) 549. https://doi.org/10.4162/nrp.2022.16.5.549.

[25] F. Santilli, M.T. Guagnano, N. Vazzana, et al., Oxidative stress drivers and modulators in obesity and cardiovascular disease: from biomarkers to therapeutic approach, Curr Med Chem. 22 (2015) 582-95. https://doi.org/10.2174/0929867322666141128163739.

[26] P.P. Sharma, V. Baskaran, Polysaccharide (laminaran and fucoidan), fucoxanthin and lipids as functional components from brown algae (Padina tetrastromatica) modulates adipogenesis and thermogenesis in diet-induced obesity in C57BL6 mice, Algal Research. 54 (2021) 102187. https://doi.org/10.1016/j.algal.2021.102187.

[27] Y. Li, J. Huang, S. Zhang, et al., Sodium alginate and galactooligosaccharides ameliorate metabolic disorders and alter the composition of the gut microbiota in mice with high-fat diet-induced obesity, Int J Biol Macromol. 215 (2022) 113-122. https://doi.org/10.1016/j.ijbiomac.2022.06.073.

[28] A. Bhattacharyya, R. Chattopadhyay, S. Mitra, et al., Oxidative stress: An essential factor in the pathogenesis of gastrointestinal mucosal diseases, Physiol Rev. 94 (2014) 329-354. https://doi.org/10.1152/physrev.00040.2012.

[29] B. Remund, B. Yilmaz, C. Sokollik, D-Lactate: Implications for gastrointestinal giseases, Children. 10 (2023) 945. https://doi.org/10.3390/children10060945.

[30] B. Lee, K.M. Moon, C.Y. Kim, Tight junction in the intestinal epithelium: Its association with diseases and regulation by phytochemicals, J Immunol Res. 2018 (2018) 1-11. https://doi.org/10.1155/2018/2645465.

[31] M. Hussain, M. Umair Ijaz, M.I. Ahmad, et al., Meat proteins in a high-fat diet have a substantial impact on intestinal barriers through mucus layer and tight junction protein suppression in C57BL/6J mice, Food Funct. 10 (2019) 6903-6914. https://doi.org/10.1039/C9FO01760G.

[32] J.K. Gustafsson, M.E.V. Johansson, The role of goblet cells and mucus in intestinal homeostasis, Nat Rev Gastro Hepat. 19 (2022) 785-803. https://doi.org/10.1038/s41575-022-00675-x.

[33] J.M. Monk, W. Wu, D. Lepp, et al., Navy bean supplemented high-fat diet improves intestinal health, epithelial barrier integrity and critical aspects of the obese inflammatory phenotype, J Nutr Biochem. 70 (2019) 91-104. https://doi.org/10.1016/j.jnutbio.2019.04.009.

[34] K. Frazier, A. Kambal, E.A. Zale, et al., High-fat diet disrupts REG3γ and gut microbial rhythms promoting metabolic dysfunction, Cell Host Microbe. 30 (2022) 809-823. https://doi.org/10.1016/j.chom.2022.03.030.

[35] Q. Luo, A. Jahangir, J. He, et al., Ameliorating effects of TRIM67 against intestinal inflammation and barrier dysfunction induced by high fat diet in obese mice, Int J Mol Sci. 23 (2022) 7650. https://doi.org/10.3390/ijms23147650.

[36] A. Medina-Larqué, M. Rodríguez-Daza, M. Roquim, et al., Cranberry polyphenols and agave agavins impact gut immune response and microbiota composition while improving gut barrier function, inflammation, and glucose metabolism in mice fed an obesogenic diet, Front Immunol. 13 (2022). https://doi.org/10.3389/fimmu.2022.871080.

[37] H. Thomas, Intestinal homeostasis is reliant on self-maintaining macrophages, Nat Rev Gastro Hepat. 15 (2018) 656-657. https://doi.org/10.1038/s41575-018-0074-x.

[38] L.M. Hegarty, G. Jones, C.C. Bain, Macrophages in intestinal homeostasis and inflammatory bowel disease, Nat Rev Gastro Hepat. 20 (2023) 538-553. https://doi.org/10.1038/s41575-023-00769-0.

[39] T.C. Moreira Lopes, D.M. Mosser, R. Gonçalves, Macrophage polarization in intestinal inflammation and gut homeostasis, Inflamm Res. 69 (2020) 1163-1172. https://doi.org/10.1007/s00011-020-01398-y.

[40] Z.Y. Li, L.H. Lin, H.J. Liang, et al., Lycium barbarum polysaccharide alleviates DSS-induced chronic ulcerative colitis by restoring intestinal barrier function and modulating gut microbiota, Ann Med. 55 (2023) 2290213. https://doi.org/10.1080/07853890.2023.2290213.

[41] S. Terzo, A. Amato, P. Calvi, et al., Positive impact of indicaxanthin from *Opuntia ficus*-indica fruit on high-fat diet–induced neuronal damage and gut microbiota dysbiosis, Neural Regen Res (2026) 324-332. https://doi.org/10.4103/nrr.nrr-d-23-02039.

[42] N. Li, X. Liu, J. Zhang, et al., Preventive effects of anthocyanins from *Lyciumruthenicum murray* in high-fat diet-induced obese mice are related to the regulation of intestinal microbiota and inhibition of pancreatic lipase activity, Molecules. 27 (2022) 2141. https://doi.org/10.3390/molecules27072141.